ILASS-Americas 22nd Annual Conference on Liquid Atomization and Spray Systems, Cincinnati, OH, May 2010

A Prediction of Primary Atomization for a Subsonic Spray in Crossflow Using the $\Sigma - Y$ Model

Nathaniel Trask*and David P. Schmidt
Department of Mechanical and Industrial Engineering
University of Massachusetts, Amherst, MA 01003

Abstract

The prediction of spray formation occuring when a liquid jet is injected normally to a high velocity gas stream is of fundamental interest to a variety of combustion and power related applications. Of primary interest is the penetration of this liquid jet and the characteric droplet diameter of the resulting spray. The $\Sigma - Y$ model for primary atomization has proven successful in predicting a number of high-velocity diesel and coaxial type injection arrangements, but has yet to be tested in more complex flow configurations. Evaluating the model's generality in predicting arbitrary injection configurations is fundamental in gauging its potential as a practical engineering tool. Encouraging preliminary results presenting the models ability to predict mass distribution and spray penetration of sprays in crossflow are presented and compared to experimental PDPA measurements.

*Corresponding Author: nat.trask@gmail.com

Introduction

The quality of atomization and its effect upon the subsequent evaporation and mixing of fuel occuring within combustion systems is fundamental in determining both the combustion efficiency and the production of emissions for a given system. In particular, the transverse injection of a liquid jet into a high velocity crossflowing gas is common in a variety of fuel injection schemes, such as the fuel injection process for lean premixed prevaporized (LPP) gas turbine engines, augmentors, and for ramjet and scramjet applications [1, 2, 3, 4, 5, 6, 7]. For these applications, crossflow injection has the desirable benefit of achieving rapid fuel atomization with control over the location of fuel placement. Of particular value to design engineers is the possibility of a predictive tool for determining the penetration of the resulting spray to prevent impingement of liquid fuel upon walls, and for determining the resulting spray atomization quality, both of which are prerequisite for modeling fuel vaporization and subsequent combustion processes.

The process by which liquid disintegrates into droplets upon injection from an orifice under conditions typical of gas turbine injection is as follows [3]: directly after injection, the liquid jet forms a column subjected to a drag force which bends to align with the coflowing gas. At the same time, the pressure distribution across the liquid interface causes the jet to adopt a flattened profile. Progressing down the length of the jet, the profile continually flattens until it becomes subject to wave-like instabilities and eventually pinches off to form ligaments oriented transversely to the flow. This breakup mechanism is referred to as column breakup and qualitatively resembles the first wind-induced regime of jet atomization. While this mechanism is predominant at lower momentum ratios, for high pressure flows typical of those found in combustors a second mechanism refered to as surface breakup occurs. Surface breakup is characterized by the high Weber number stripping of ligaments by shear forces acting at the liquid surface and tends to form smaller droplets than the column breakup mechanism. The ligaments formed by both mechanisms then undergo secondary breakup typically driven by shear breakup mechanisms [8].

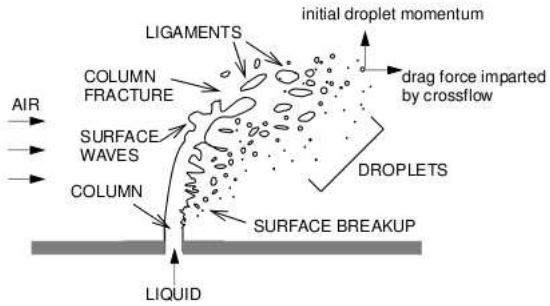

Figure 1: Schematic representing the two mechanisms of primary atomization and subsequent transition to secondary breakup. [1]

Experimental work has been conducted to characterize maps of the two breakup regimes, and corellations for jet trajectory, penetration, and jet width. For much of the experimental work at high Weber number and momentum ratio, the cloud of small droplets formed by the surface breakup process (Figure 2) render the primary atomization zone and point of jet breakup optically inaccesible. The majority of published experimental work utilizes either a shadowgraphy or Phase Dopppler and Particle Analyzer (PDPA) technique to characterize the breakup zone. Shadowgraphy fails to resolve spray regions of small droplet density, and as a result tend to yield shorter jet penetrations than PDPA experiments [2] [9]. Promising work has recently been conducted by Linne et al. [6] using ballistic imaging techniques to resolve both the small scale features occuring due to surface breakup and large scale, periodic features of the primary liquid core.

Figure 2: Droplets from surface breakup mechanism visually obscure the primary liquid core. [2]

Of all the numerical approaches typically used to model atomization processes, the Lagrangian "blob" formulation employed by Reitz [10] is probably the most ubiquitous and is readily implemented in a number of commercial CFD packages. While this framework has given excellent agreement in cases where a liquid jet is injected into either quiescent

or coflowing gas, the assumption that the gas and liquid phases are only coupled through momentum transfer is inadequate to resolve the jet in crossflow behaviour. The wake formed by the presence of the liquid column alters the turbulent structures (Figure 3). Also, to the leeward side of the jet there is a low pressure zone similar to that found in the wake of a solid cylinder that contributes to the bending of the liquid column.

A number of other modeling approaches have been carried out in the literature. Bellofiore et al. coupled an Eulerian analysis of the jet to a Boundary Layer Stripping model to predict the depletion of mass from the jet due to stripping, obtaining good predictions of penetration and trajectory at high jet velocities [11]. Mashayek and Ashgritz developed an analytic-numerical model of the spreading of the jet via an analogy to the deformation of a liquid droplet in quasi-static liquid flow [12] and were able to reproduce results from experimental photographs of the jet deformation at low momentum ratios.

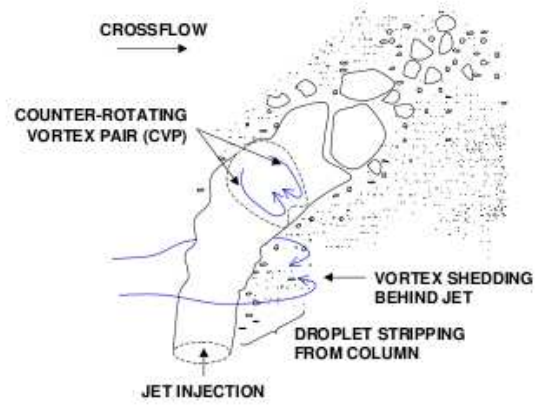

Figure 3: Effect of liquid column on surrounding turbulent structures. [13]

The $\Sigma - Y$ model, originally proposed by Borghi and Vallet [14], attempts to capture the features of the flow of practical interest to the design engineer while simplifying the complexities of the flow via simple closures within an Eulerian framework. By recasting the governing equations of motion in a Reynolds averaged paradigm, the bulk liquid movement is predicted. Rather than attempting to resolve individual atomization events, a transport equation for the development of surface tension energy is used to characterize the rate at which surface area is created. With knowledge of a local interfacial surface area and liquid volume, the Sauter mean diameter can then be characterized. Predictions for the mean droplet size and spatial distribution can then be used as an input for Lagrangian secondary breakup models which can be used to predict fuel vaporization, which in turn provide the necessary inputs for combustion calculations. The $\Sigma - Y$ model has been successfully applied and validated for a variety of coaxial and diesel jet type injections [15, 16, 17, 18, 19] and recently used for injection schemes with more complex geometries [20].

For this work, the accuracy of the $\Sigma - Y$ model in reproducing the liquid trajectory and liquid volume distribution given by the work of Tambe et al. [2] will be evaluated. Tambe's experimental work investigated the effects of altering momentum ratio, freestream velocity, nozzle diameter, and surface tension coefficient upon the structure of the resulting atomized spray.

Methodology

The $\Sigma - Y$ modeling approach applied in this paper, originally developed by Borghi and Vallet, employs the following assumptions:

- Surface tension and viscosity act only at small length scales, which corresponds to the limit of infinite Reynolds and Weber numbers. This implies that the large scale features of the flow will be dependent only upon density variations and bulk momentum transport. The surface tension and viscosity will only have an effect upon subgrid scale flow features. Tambe's suggestion that surface tension effects only droplet size and not penetration supports this assumption [2].

- Although the small scale velocity fluctuations of the flow are unpredictable at the desired resolutions, the effect of the mean velocity field can be predicted using standard turbulence closures, such as the classical two equation k-epsilon model.

- The dispersion of the liquid phase into the gaseous phase can be modeled via a turbulent diffusion flux.

- The mean geometry of the liquid structures can be characterized by tracking the mean surface area of the liquid-gas interface per unit volume. This is equivalent to tracking the transfer of kinetic energy to surface tension potential energy.

To track the dispersion of the liquid phase an indicator function Y is introduced with value 1 in the liquid phase and 0 in the gas phase. The mean

liquid volume fraction of the fluid is then defined as $\bar{Y}$, and the mean mass averaged fraction is defined as $\tilde{Y} = \frac{\overline{\rho Y}}{\bar{\rho}}$. The transport equation for $\tilde{Y}$ then takes the form:

$$\frac{\partial \bar{\rho}\tilde{Y}}{\partial t} + \frac{\partial \bar{\rho}\tilde{u}_i\tilde{Y}}{\partial x_j} = -\frac{\partial \bar{\rho}\widetilde{u_i'Y'}}{\partial x_i} \tag{1}$$

where u' denotes the density weighted turbulent fluctuations in velocity and Y' denotes turbulent fluctuations in volume fraction.

The value of $\tilde{Y}$ is related to ρ by

$$\frac{1}{\rho} = \frac{\tilde{Y}}{\rho_{liq}} + \frac{1-\tilde{Y}}{\rho_{gas}} \tag{2}$$

Under the assumption that viscous effects only contribute to the small scale motion of the flow, the momentum equation for the bulk fluid motion is given by the equation:

$$\frac{\partial \bar{\rho}\tilde{u_j}}{\partial t} + \frac{\partial \bar{\rho}\tilde{u_i}\tilde{u_j}}{\partial x_i} = -\frac{\partial \bar{p}}{\partial x_j} - \frac{\partial \bar{\rho}\widetilde{u_i u_j}}{\partial x_i} \tag{3}$$

These equations have two unclosed terms that must be modeled: the turbulent diffusion liquid flux $\widetilde{u_i'Y'}$ capturing the effect of the relative velocity between the liquid and gas phases, and the Reynolds stress tensor $\widetilde{u_i u_j}$ capturing the momentum dissipation imposed upon the mean flow by the velocity fluctuations.Closure of the Reynolds stress tensor in the momentum equation has traditionally been obtained through a classical $k-\epsilon$ model, although Demoulin proposes a modification of the two-equation model to account for the enhanced production of kinetic energy caused by the large density gradients typical of atomization processes. For this work, the realizable $k-\epsilon$ model proposed by [21] was employed, as it has been shown to better resolve the dissipation of kinetic energy in the wake caused by flows past obstacles. To close the turbulent diffusion liquid flux term, a simple turbulent diffusion hypothesis has been shown to yield good results far from the primary atomization zone. For primary atomization processes Demoulin et al. proposed the following term capturing the enhancement of liquid mixing caused by accelerating large density gradients via a Rayleigh-Taylor type mechanism.

$$\bar{\rho}\widetilde{u'_i Y'} = \rho\left[\frac{\nu_t}{Sc} + C_p\frac{k^2}{\epsilon}\bar{\rho}\left(\frac{1}{\rho_g} - \frac{1}{\rho_l}\right)\tilde{Y}(1-\tilde{Y})\right]\frac{\partial \tilde{Y}}{\partial x_i} \tag{4}$$

This term has been implemented in the present work, where the modeling constants Sc and C_p are set to 0.9 and 1.8, respectively. These values are consistent with those previously used in the literature for coaxial and diesel jets.

The system is closed by assuming an incompressible equation of state for the liquid phase and a perfect gas law for the gas phase, yielding the following relation for the mean density:

$$\frac{1}{\rho} = \frac{\tilde{Y}}{\rho_{liq}} + \frac{(1-\tilde{Y})R_g T}{p} \tag{5}$$

The temperature can either be determined through the solution of a transport equation for internal energy or enthalpy, or by assuming the gas to be isothermal. For the moderate Mach numbers considered in this study thermal compressibility effects were neglected.

These equations were solved using the open source finite volume C++ library OpenFOAM [22]. OpenFOAM provides the framework for rapidly constructing fully parallelized, three-dimensional solvers for general polyhedral meshes. Because OpenFOAM operates in a fully segregated paradigm, a PISO algorithm is used to achieve coupling between the momentum and continuity equations [23]. The PISO algorithm operates by:

- Using the pressure from the previous timestep to solve the momentum equation. This gives a non-conservative predictor for the velocity fluxes.
- Solving a pressure equation to correct the velocity fluxes and force them to obey the continuity equation.
- Iterate using the most recent value of pressure to account for nonlinear effects.

In order to do this, a transport equation for pressure must be derived. The momentum equation is recast in a semi-discretized form:

$$a_p\mathbf{U}_p = \mathbf{H}(\mathbf{U}) - \nabla p \tag{6}$$

where $\mathbf{H(u)}$ consists of two parts: the advection terms which includes the matrix coefficients of neighboring cells multiplied by the corresponding velocities and the source term, accounting for all point sources in the momentum equations (such as gravity, body forces, etc.).

$$\mathbf{H}(\mathbf{U}) = \sum_N a_N\mathbf{U}_N + \frac{\mathbf{U}^0}{\Delta t} \tag{7}$$

Equation 6 is rearranged and interpolated to faces. Taking the divergence of this gives

$$\nabla \cdot (\mathbf{U}_p)_f = \nabla \cdot \phi^* - \nabla \cdot \left(\frac{1}{a_p} \nabla p \right)_f \tag{8}$$

Where ϕ^* is the value of the velocity fluxes obtained from the predictor step. The velocity divergence can be split between the effects of turbulent mixing and compressibility effects by applying the chain rule to the continuity equation.

$$\nabla \cdot (\mathbf{U}_p)_f = -\frac{1}{\rho} \frac{\partial \rho}{\partial \tilde{Y}} \frac{D\tilde{Y}}{Dt} - \frac{1}{\rho} \frac{\partial \rho}{\partial \tilde{p}} \frac{D\tilde{p}}{Dt} \tag{9}$$

where $\frac{\partial \rho}{\partial \tilde{p}}$ is the isothermal compressibility ψ which is determined by taking the partial of Equation 2 with respect to ρ, giving

$$\psi = \left(\frac{\rho}{\rho_g} \right)^2 \frac{1 - \overline{Y}}{R_g T} \tag{10}$$

After some rearrangement, combining Equation 9 with Equations 1 and 10 gives:

$$\nabla \cdot \left(\frac{1}{a_p} \mathbf{H}(\mathbf{U})_f \right) - \nabla \cdot \phi^* = \frac{1 - \overline{Y}}{p} \frac{Dp}{Dt} + \left(\frac{1}{\rho_l} - \frac{1}{\rho_g} \right) \bar{\rho} \widetilde{u'_i Y'} \tag{11}$$

Using this updated pressure to correct the fluxes will give a velocity field that satisfies the continuity equation. To correct for nonorthogonality effects and nonlinearities in the pressure equation, this process of solving Equation 11 and updating the fluxes can be repeated iteratively until a suitable tolerance is reached.

Case Setup

The experimental conditions investigated by Tambe et al. [2] were matched to determine the $\Sigma - Y$ model's ability to predict mass distribution for sprays in crossflow. Tambe investigated injections of water, Jet-A, and N-Heptane and the effect of varying injection diameter, momentum ratio, crossflow velocity, and surface tension coefficient in the downstream liquid mass flux and Sauter mean diameter profiles. In their work they noted that increasing the surface tension coefficient had little effect upon the penetration of the liquid jet, and only served to increase the resulting droplet size resulting from surface breakup. This suggests that the hypothesis of the $\Sigma - Y$ model that the bulk fluid motion remains separate from the breakup behaviour should be satisfied for this case.

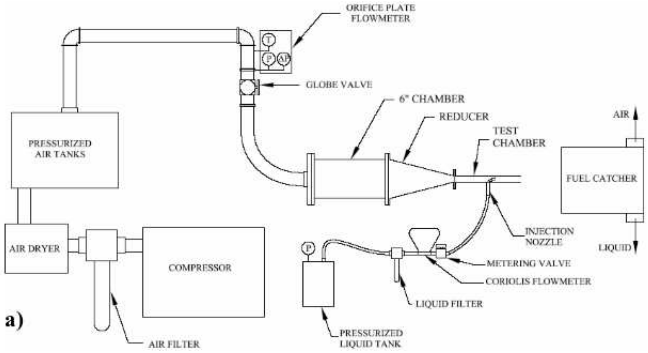

Figure 4: Experimental setup used by Tambe et al. [2]

Figure 4 shows the experimental setup used by Tambe et al. [2]. For this numerical investigation, the test chamber following the reducer throat was simulated using a hexahedral mesh of 500k cells. The mesh was refined in the vicinity of the liquid jet and near the boundary layer at the lower wall such that the characteristic cell size in the vicinity of the injector and within the boundary layer was 70 microns. The mesh far from domain occupied by the liquid jet was coarsened to increase computational efficiency. The operating conditions modeled are given in Table 1. Uniform turbulent boundary conditions were imposed to match fully developed turbulent pipe flow conditions of an equivalent hydraulic diameter. Experimental evidence suggests that it is necessary to resolve momentum boundary layer effects [24, 2]. Wall functions were applied to obtain turbulent boundary layer characteristics. The momentum boundary layer was modeled at the inlet using the following relations for a turbulent boundary layer over a flat plate.

$$\frac{\delta}{L} = \frac{0.37}{Re^{\frac{1}{5}}} \tag{12}$$

$$\frac{u}{U_{\text{inf}}} = \left(\frac{y}{\delta} \right)^{\frac{1}{7}} \tag{13}$$

where δ denotes the boundary layer thickness and Re is the Reynolds number based on the streamwise plate length. This length was taken to be the distance from the end of the reducer to the beginning of the simulated domain (10 cm), giving a boundary layer thickness at the beginning of the computational domain of 2.5 mm.

Table 1: Simulation conditions

Case number	5
Liquid	Water
D (mm)	0.381
We	96.2
Momentum ratio	5.2
$U_\infty(\frac{m}{s})$	123.1
$U_{liq}(\frac{m}{s})$	9.7
p_∞ kPa	101.325

Figure 5: Shadowgraph of spray structure for case 5 by Tambe et al. [2]

As seen in Figure 6, the simulation captures a number of the relevant qualitative flow features. A relatively solid primary liquid core forms with a lesser amount of mass in its wake, corresponding to the expected high Weber number mixing caused by the shear-driven surface breakup. A comparison of the results to measurements of normalized liquid volume flux and Sauter mean diameter 30 inlet diameters downstream of the injection point (Figures 6 - 8) show reasonable agreement in mass placement and location of interfacial surface area. While it is not possible to directly compare values of volume fraction due to the fact that Tambe et al. only published volume fluxes normalized by their maximum value, the results do indicate that the majority of mass is within 6 mm of the wall. Of particular relevance is the fact that this level of agreement has been achieved using the exact same values as those used to predict coaxial and diesel jet injections. Previous work [20] has shown that altering either the Schmidt number or the constant C_p found in Equation 4 can be used to better fit experimental values for the position of the primary liquid core.

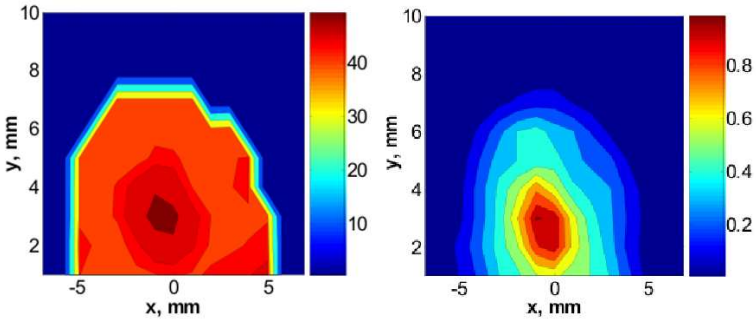

Figure 6: Experimental measurements of SMD (left) and liquid volume flux (right) [2]

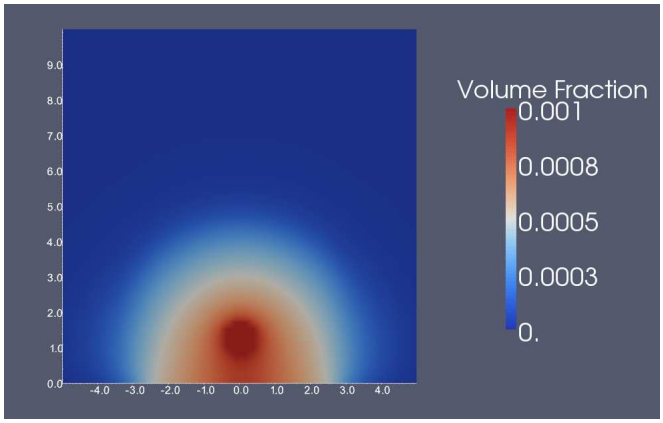

Figure 7: Liquid volume fraction measured 30 diameters downstream of liquid inlet.

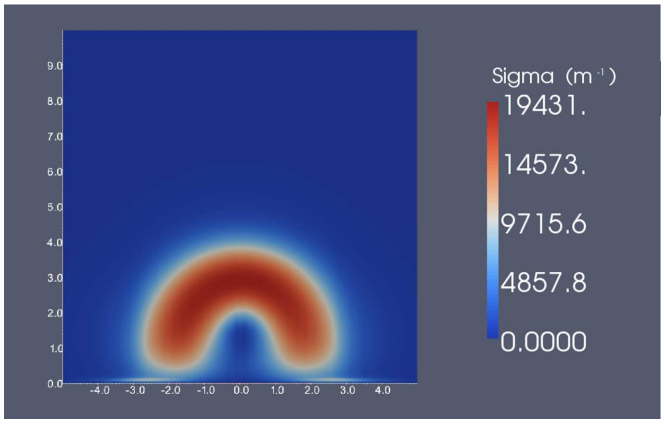

Figure 8: Interfacial surface area density measured 30 diameters downstream of liquid inlet.

Figures 9 and 10 compare the results of the simulation to empirical correlations for spray penetration cited in [2]. The differences between the

correlations have been attributed by Tambe et al. to both differences in experimental techniques between studies and differences in ambient operating conditions. While the penetration of the primary liquid core is significantly less than that predicted by the correlations, the outer sparse region of the spray containing the majority of the interfacial surface area shows excellent agreement.

Conclusions

The $\Sigma - Y$ model for predicting primary atomization has shown to give promising preliminary results in predicting atomization in spray in crossflow injection schemes with no alteration of the model. This is particularly encouraging, as previous work with the model has focused primarily upon simple shear driven atomization arrangements. Additional work is required to determine the generality of the model and whether better accuracy can be obtained through the use of more suitable modeling parameters.

The results are additionally encouraging for design engineers looking for practical tools for predicting atomization. Unlike most atomization models, the $\Sigma - Y$ model has been shown here to provide reasonably accurate predictions with no a priori knowledge of the flow. Work is currently underway to couple this primary atomization model to a Lagrangian model for secondary breakup using the so-called Eulerian-Lagrangian Spray Atomization (ELSA) framework [25] which will allow better prediction of spray behaviour as the flow becomes sparse.

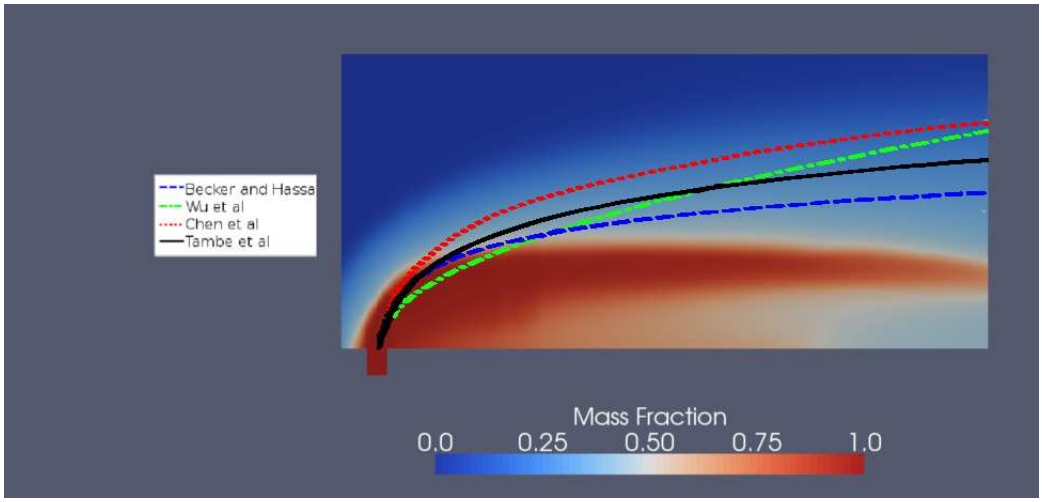

Figure 9: Predicted liquid mass fraction with superimposed correlations of spray penetration [26, 27, 28].

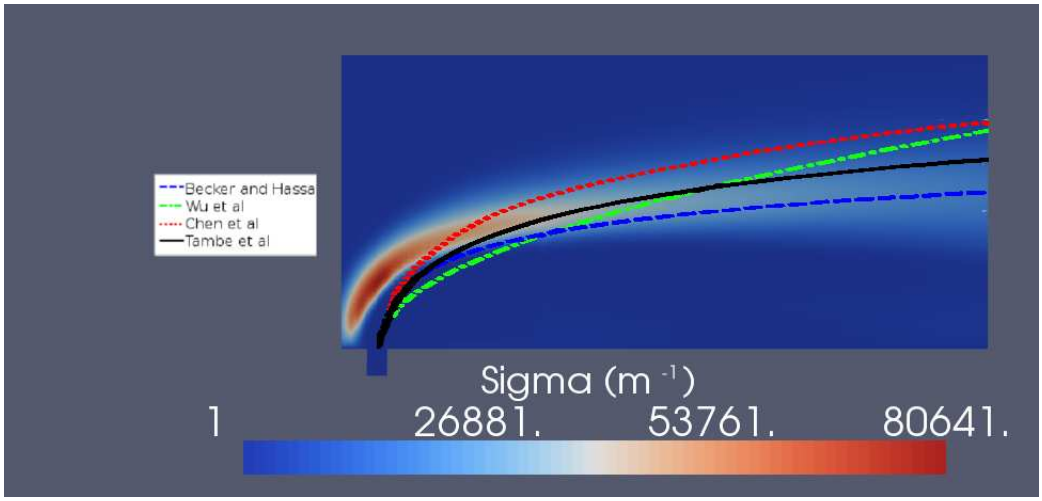

Figure 10: Predicted interfacial surface area density with superimposed correlations of spray penetration [26, 27, 28].

References

[1] P.-K. Wu, K.A. Kirkendall, R.P. Fuller, and A.S. Nejad. *Journal of Propulsion and Power*, 13:64–73, 1997.

[2] S. Tambe, S. Jeng, M. Mongia, and G. Hsiao. *43rd AIAA Aerospace Sciences Meeting and Exhibit*, Reno, Nevada, January 2005.

[3] M. Rachner, J. Becker, C. Hassa, and T. Doerr. *Aerospace Science and Technology*, 6:495–506, 2002.

[4] T. Inamura, N. Nagai, T. Hirai, and H. Asano. *Proceedings of the 5th International Conference on Liquid Atomization and Spray Systems*, Gaithersberg, MD, USA, 1991.

[5] T. Inamura and N. Nagai. *Journal of Propulsion and Power*, 13:250–256, 1997.

[6] M.A. Linne, M. Paciaroni, J. R. Gord, and T.R. Meyers. *Applied Optics*, 44:6627–6634, 2005.

[7] R. Ragucci, A. Bellofiore, and A. Cavaliere. *Proceedings of the Combustion Institute*, 31:2231–2238, 2007.

[8] A.A. Ranger and J.A. Nicholls. *AIAA Journal*, 7:285–290, 1969.

[9] K.C. Lin, P.J. Kennedy, and T.A. Jackson. *Proceedings of the 15th International Conference on Liquid Atomization and Spray System*, Madison, Wisconsin USA, 2002.

[10] R.D. Reitz. *Atomization Spray Technology*, 3:309–337, 1987.

[11] A. Bellofiore, P. Di Martino, A. Cavaliere, and R. Ragucci. *Proceedings of the European Combustion Meeting 2005*, 2005.

[12] A. Mashayek and N. Ashgriz. *AIAA Journal*, 47, 2009.

[13] M. Y. Leong, V. G. McDonell, and G. S. Samuelsen. Mixing of an airblast-atomized fuel spray injected into a crossflow of air. Technical Report NASA/CR-2000-210467, National Aeronautics and Space Administration, 2000.

[14] A. A. Burluka, A. Vallet, and R. Borghi. *Atomization and Sprays*, 11:619–642, 2001.

[15] N. Meyers, F. Dupoirieux, and M. Habiballah. *Proc. 1st Eur. Conf. Aerosp. Sci.*, 2005.

[16] F. Lacas, S. Jay, and S. Candel. *Combustion and Flame*, 144:558–577, 2001.

[17] N. Beheshti, A. Burluka, and M. Fairweather. *Theoretical and Computational Fluid Dynamics*, 21:381–397, 2007.

[18] W. Ning, R.D. Reitz, R. Diwakar, and A.M. Lippert. *SAE SP*, 2183:129–152, 2008.

[19] T. Menard, P.A. Beau, A. Berlemont, R. Lebas, and F.X. Demoulin. *International Journal of Multiphase Flow*, 35:247–260, 2009.

[20] N. Trask, J.B. Perot, D.P. Schmidt, T. Meyer, M. Lightfoot, and S. Danczyk. *48th AIAA Aerospace Sciences Meeting Including the New Horizons Forum and Aerospace Exposition*, 2010.

[21] T.H. Shih, W.W. Liou, A. Shabbir, Z. Tang, and J. Zhu. *Computers and Fluids*, 24:227–238, 1995.

[22] H. G. Weller, G. Tabor, H. Jasak, and C. Fureby. *Computers in Physics*, 12(6):620–63, 1998.

[23] J.H. Ferziger and M. Peric. *Computational methods for fluid dynamics*. Springer, Berlin, 2002.

[24] L. J. Chelko. Penetration of liquid jets into a high-velocity air stream. Technical Report NACA RM E50F21, National Advisory Committee for Aeronautics, 1950.

[25] R. Lebas, G. Blokkeel, P.A. Beau, and F.X. Demoulin. *SAE Technical Papers*, April 2005.

[26] J. Becker and C. Hassa. *Atomization and Sprays*, 11:49–67, 2002.

[27] P.-K. Wu, K.A. Kirkendall, R.P. Fuller, and A.S. Nejad. *Journal of Propulsion and Power*, 14:173–181, 1998.

[28] T.H. Chen, C.R. Smith, and D.G. Schommer. Multi-zone behaviour of transverse liquid jet in high-speed flow. Technical Report Paper 93-0453, AIAA, 1993.